3 Non-linear Elasticity

3.1 Deformation Gradient and Stress-Stretch Relation

In Fig. 3.1 we illustrate the motion of a body from a stress-free reference state, in which a material particle lies at x_i^0, to a deformed state, − occupied at time t − where the particle lies at x_i. We may describe the motion of the particle by the function

$$x_i = x_i(x_j^0, t). \tag{3.1}$$

Two adjacent material particles are connected by the line elements $\mathrm{d}x_i^0$ and $\mathrm{d}x_i$ respectively, in the two states and (3.1) implies

$$\mathrm{d}x_i = \frac{\partial x_i}{\partial x_j^0}\mathrm{d}x_j^0 \quad \text{or, with} \quad F_{ij} \equiv \frac{\partial x_i}{\partial x_j^0}: \quad \mathrm{d}x_i = F_{ij}\mathrm{d}x_j^0. \tag{3.2}$$

F_{ij} is called the deformation gradient. In an elastic body F_{ij} determines the stress t_{ij}.

Therefore we may write

$$t_{ij} = \tau_{ij}\left(F_{kl}\right). \tag{3.3}$$

This relation is known at the stress-deformation relation of elasticity. It consists of six independent equations, since the stress tensor t_{ij} is symmetric.

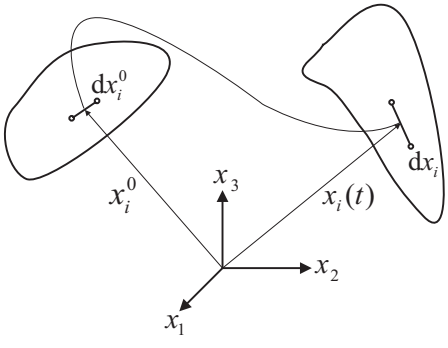

Fig. 3.1. Motion of a body and deformation of a line element

I. Müller and P. Strehlow: *Rubber and Rubber Balloons, Paradigms of Thermodynamics*, Lect. Notes Phys. **637**, (2004), pp. 21–34
http://www.springerlink.com/

The functions τ_{ij} determine how the stress is related to the deformation gradient; they depend on the "constitution" of the elastic material, meaning that it is different for steel, aluminium, rubber, etc. Therefore the functions τ_{ij} are called constitutive functions and (3.3) is called a constitutive relation.

We proceed to determine properties of the constitutive function for a material which is isotropic.

3.2 Material Symmetry and Isotropy

We apply the same stress t_{ij} to an originally stress-free body in two different reference states with line elements $\mathrm{d}x_i^0$ and $\mathrm{d}x_i^{\hat{0}}$ such that at time t the line elements $\mathrm{d}x_i$ are equal, see Fig. 3.2.

The line elements $\mathrm{d}x_i^0$ and $\mathrm{d}x_i^{\hat{0}}$ are not generally equal because the body may be softer in the direction of the applied force in state 0 than in state $\hat{0}$. That is indeed the situation depicted in the figure, where the hard direction is indicated by the parallel lines. Since the stresses are equal and the deformation gradients are not equal, the constitutive functions must be different and we denote them by ${}_0\tau_{ij}$ and ${}_{\hat{0}}\tau_{ij}$. The two functions are related by the equation, cf. Fig. 3.2

$$ {}_{\hat{0}}\tau_{ij}\,(F_{kl}) = {}_0\tau_{ij}(F_{kn}P_{nl}), \qquad \text{where} \qquad P_{nl} = \frac{\partial x_n^{\hat{0}}}{\partial x_l^0}. \tag{3.4} $$

The matrix P_{nl} may be interpreted as the deformation gradient between state 0 and state $\hat{0}$. It follows from (3.4) that the constitutive functions ${}_{\hat{0}}\tau_{ij}$ can be determined from knowledge of the functions ${}_0\tau_{ij}$.

All this has nothing to do with material symmetry or isotropy. The preceding arguments are only preparatory to the discussion of symmetry which follows *now*.

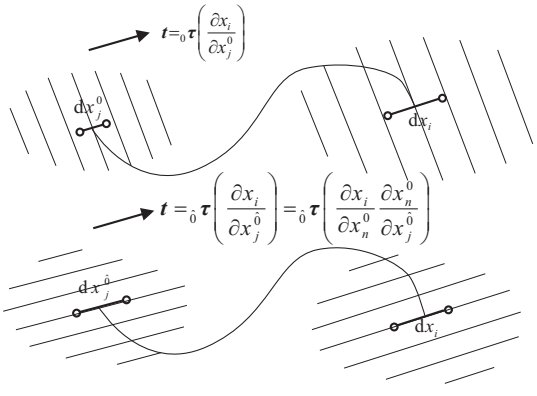

Fig. 3.2. Same stress applied to different reference states so that deformed states agree

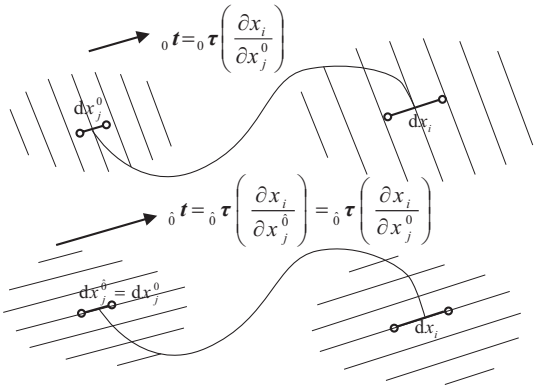

Fig. 3.3. Same deformation gradient applied to different reference states generally requires different stresses

In Fig. 3.3 we again have the reference states 0 and $\hat{0}$ and now we look at identical line elements $\mathrm{d}x_i^0$ and $\mathrm{d}x_i^{\hat{0}}$ to which we apply the same deformation, so that at time t they are both given by the same element $\mathrm{d}x_i$. In general the necessary stresses will be different due to the difference of soft and hard directions, viz.

$$ {}_0t_{ij} = {}_0\tau_{ij}\left(F_{kl}\right) \qquad \text{and} \qquad {}_{\hat{0}}t_{ij} = {}_{\hat{0}}\tau_{ij}\left(F_{kl}\right). \tag{3.5}$$

However, if the stresses are *equal* we say that the body is *symmetric* with respect to the transformation $\boldsymbol{P}$ from state 0 to state $\hat{0}$. By (3.5) the condition of symmetry thus reads

$$ {}_0\tau_{ij}\left(F_{kl}\right) = {}_{\hat{0}}\tau_{ij}\left(F_{kl}\right), \quad \text{or by (3.4)} \quad {}_0\tau_{ij}\left(F_{kl}\right) = {}_0\tau_{ij}\left(F_{kn}P_{nl}\right). \tag{3.6}$$

If this condition of symmetry holds for all rotations so that $\boldsymbol{P}$ in $(3.6)_2$ can be any proper orthogonal matrix $\boldsymbol{O}$, we say that the body is *isotropic*. The condition of symmetry thus reads

$$ t_{ij} = {}_0\tau_{ij}\left(F_{kl}\right) = {}_0\tau_{ij}\left(F_{kn}O_{nl}\right). \tag{3.7}$$

Therefore in a symmetric body the stress is unaffected when the deformation gradient $\boldsymbol{F}$ is replaced by $\boldsymbol{FO}$. Another way of saying this is that the stress can only depend on such combinations of F_{ij} that are invariant under the replacement of $\boldsymbol{F}$ by $\boldsymbol{FO}$. The stretch tensor $\boldsymbol{B} = \boldsymbol{FF}^{\mathrm{T}}$ is such a combination – because we have $\boldsymbol{FO}\left(\boldsymbol{FO}\right)^{\mathrm{T}} = \boldsymbol{FF}^{\mathrm{T}}$. A little reflection shows that it is the most general one. Therefore the generic constitutive relation of an isotropic elastic body reads

$$ t_{ij} = \tau_{ij}\left(B_{kl}\right). \tag{3.8}$$

Comparing (3.8) with (3.3) we see that isotropy considerably simplifies the constitutive equation of an elastic body. Thus, while F_{kl} has 9 components, B_{kl} has only 6 independent components since $\boldsymbol{B}$ is symmetric.

3.3 Material Objectivity

Material objectivity means that the constitutive functions – here τ_{ij} – have the same form for an elastic body in any inertial or non-inertial frame. We may express this by saying that a given stretch produces the same stress irrespective of whether a body lies at rest in the laboratory or on a carrousel. However, the *components* of stress and stretch are different in the two frames. We have

$$t^*_{ij} = O_{ik} t_{kl} O^{\mathrm{T}}_{lj} \qquad \text{and} \qquad B^*_{ij} = O_{ik} B_{kl} O^{\mathrm{T}}_{lj}, \tag{3.9}$$

when the starred quantities are the components referred to the carrousel and O_{ik} is the matrix of rotation of the carrousel axes with respect to those in the laboratory.

Thus material objectivity requires

$$t^*_{ij} = \tau_{ij}\left(B^*_{rs}\right) \qquad \text{and} \qquad t_{ij} = \tau_{ij}\left(B_{rs}\right). \tag{3.10}$$

Note that the functions are equal in both equations. Combining these equations we obtain by use of (3.9)

$$O_{ik}\tau_{kl}\left(B_{rs}\right) O^{\mathrm{T}}_{lj} = \tau_{ij}\left(O_{rk} B_{kl} O^{\mathrm{T}}_{ls}\right) \tag{3.11}$$

and this must hold for all proper orthogonal matrices $\boldsymbol{O}$. We express this condition by saying that τ_{ij} is an isotropic tensorial function.[1] Equation (3.11) represents a functional equation for τ_{ij} and we proceed to find its solution, i.e. the general form permitted by the equation.

3.4 Representation of an Isotropic Function

Since the stretch tensor $\boldsymbol{B}$ is symmetric, it can be diagonalized by an orthogonal matrix that rotates the coordinate axes into the directions of the principal axes of $\boldsymbol{B}$. In that frame – characterized by an overbar – $\boldsymbol{B}$ has the form

$$\begin{bmatrix} \bar{B}_1 & 0 & 0 \\ 0 & \bar{B}_2 & 0 \\ 0 & 0 & \bar{B}_3 \end{bmatrix}$$

and the diagonal elements are called the principal stretches. The stress in that frame is also diagonal so that we may write

$$\bar{t}_{ij} = \begin{bmatrix} \bar{t}_1 & 0 & 0 \\ 0 & \bar{t}_2 & 0 \\ 0 & 0 & \bar{t}_3 \end{bmatrix}.$$

[1] So called, because by material objectivity the constitutive relation (3.8) of an isotropic elastic body must satisfy the condition (3.11).

For proof of the diagonality of $\bar{t}_{ij}$ we write (3.11) in the frame of principal stretches as

$$O_{ik}\bar{\tau}_{kl}\left(\begin{bmatrix}\bar{B}_1 & 0 & 0\\ 0 & \bar{B}_2 & 0\\ 0 & 0 & \bar{B}_3\end{bmatrix}\right)O^{\mathrm{T}}_{lj}=\bar{\tau}_{ij}\left(O_{rk}\begin{bmatrix}\bar{B}_1 & 0 & 0\\ 0 & \bar{B}_2 & 0\\ 0 & 0 & \bar{B}_3\end{bmatrix}_{kl}O^{\mathrm{T}}_{ls}\right) \tag{3.12}$$

and we choose

$$O_{ij}=\begin{bmatrix}1 & 0 & 0\\ 0 & -1 & 0\\ 0 & 0 & -1\end{bmatrix}_{ij}.$$

Thus we have

$$O_{ij}\begin{bmatrix}\bar{B}_1 & 0 & 0\\ 0 & \bar{B}_2 & 0\\ 0 & 0 & \bar{B}_3\end{bmatrix}_{jl}O^{\mathrm{T}}_{ls}=\begin{bmatrix}\bar{B}_1 & 0 & 0\\ 0 & \bar{B}_2 & 0\\ 0 & 0 & \bar{B}_3\end{bmatrix}_{is},\ \text{hence}$$

$$\begin{bmatrix}\bar{\tau}_{11} & -\bar{\tau}_{12} & -\bar{\tau}_{13}\\ -\bar{\tau}_{12} & \bar{\tau}_{22} & \bar{\tau}_{23}\\ -\bar{\tau}_{13} & \bar{\tau}_{23} & \bar{\tau}_{33}\end{bmatrix}=\begin{bmatrix}\bar{\tau}_{11} & \bar{\tau}_{12} & \bar{\tau}_{13}\\ \bar{\tau}_{12} & \bar{\tau}_{22} & \bar{\tau}_{23}\\ \bar{\tau}_{13} & \bar{\tau}_{23} & \bar{\tau}_{33}\end{bmatrix},$$

so that $\bar{\tau}_{12}$ and $\bar{\tau}_{13}$ must vanish. $\bar{\tau}_{23}$ must also vanish; this can be concluded in an analogous manner from (3.12) by choosing

$$O_{ij}=\begin{bmatrix}-1 & 0 & 0\\ 0 & -1 & 0\\ 0 & 0 & 1\end{bmatrix}_{ij}.$$

Thus $\bar{t}_{ij}$ is indeed diagonal.

In the frame of principal stretches and − as we have now proved − of principal stresses the six independent stress-stretch relations (3.8) for an isotropic elastic body reduce to three equations, viz.

$$\bar{t}_i=\tau_i\left(\bar{B}_1,\bar{B}_2,\bar{B}_3\right)\qquad\text{for}\qquad i=1,2,3. \tag{3.13}$$

Thus only the three functions τ_i characterize the constitutive properties of an isotropic elastic material. We may replace these three functions by the triple $s_\pm$ and P by writing

$$\bar{t}_i=s_-\ \bar{B}_i^{-1}-P+s_+\bar{B}_i\qquad\text{for}\quad i=1,2,3, \tag{3.14}$$

where $s_\pm$ and P are functions of the principal stretches $\bar{B}_i$ whose form, in terms of τ_i, may be determined easily by comparison of (3.14) with (3.13).

Upon transforming back from the frame of principal stretches to an arbitrary reference frame we may write (3.14) in the form

$$t_{ij} = s_- \; B_{ij}^{-1} - P \; \delta_{ij} + s_+ \; B_{ij}. \tag{3.15}$$

This is the *representation* of an isotropic tensorial function τ_{ij} of the symmetric tensor B_{ij}.

Equation (3.15) represents the generic form of the stress-stretch relation of an isotropic body. P is called the pressure and $s_\pm$ are elastic coefficients. All three quantities must be given as functions of the principal stretches by constitutive relations. Note that the isotropy condition (3.11) has reduced the six functions τ_{ij} in (3.8) − each a function of six variables − to the three functions $s_\pm$ and P of which each one depends on three variables only.

3.5 Incompressibility. Mooney-Rivlin Material

For incompressible materials, such as rubber, the stress-stretch relation (3.15) is formally unchanged. But there are two simplifications:

An incompressible material cannot experience a volume change. Therefore the determinant of the deformation gradient $\boldsymbol{F}$, and hence the determinant of $\boldsymbol{B}$ must be equal to 1

$$\bar{B}_1 \bar{B}_2 \bar{B}_3 = 1.$$

Thus only two of the three principal stretches are independent and $s_\pm$ depend only on those two as variables.

What is more, an arbitrary pressure may be added to the stress without affecting the motion of an incompressible body. Therefore P in (3.15) is *not* a constitutive coefficient; rather it is an arbitrary function of x_i and t to be determined by boundary conditions.

A model constitutive equation for incompressible non-linear elasticity results from (3.15) by setting the elastic coefficients $s_\pm$ constant, independent of principal stretches. For that choice the stress-stretch relation is said to characterize a *Mooney-Rivlin* material. Such a constitutive equation represents a good model for the study of qualitative effects of non-linear elasticity, particularly for rubber.

Indeed, it turns out that in rubber we may set − for room temperature −

$$s_+ = 3 \text{ bar} \quad \text{and} \quad s_- = -0.3 \text{ bar} \tag{3.16}$$

and obtain fairly good results. Among those results there is a reasonable pressure-radius characteristic of a balloon as we shall show in Sect. 3.8.

Of course the elastic coefficients also depend on temperature. For rubber their dependence on temperature is linear; this reflects the entropic character of rubber elasticity.

3.6 Biaxial Stretching of a Mooney-Rivlin Membrane

We refer to Fig. 2.5 which represents a homogeneous biaxial loading of a membrane with a deformation gradient, cf. (2.32):

$$\boldsymbol{F} = \begin{bmatrix} \lambda & 0 & 0 \\ 0 & \mu & 0 \\ 0 & 0 & \frac{1}{\lambda\mu} \end{bmatrix}, \text{ hence } \boldsymbol{B} = \begin{bmatrix} \lambda^2 & 0 & 0 \\ 0 & \mu^2 & 0 \\ 0 & 0 & \frac{1}{\lambda^2\mu^2} \end{bmatrix}, \boldsymbol{B}^{-1} = \begin{bmatrix} \frac{1}{\lambda^2} & 0 & 0 \\ 0 & \frac{1}{\mu^2} & 0 \\ 0 & 0 & \lambda^2\mu^2 \end{bmatrix}. \tag{3.17}$$

Therefore, by (3.15) we have

$$\begin{bmatrix} t_{\lambda\lambda} & 0 & 0 \\ 0 & t_{\mu\mu} & 0 \\ 0 & 0 & 0 \end{bmatrix} = s_- \begin{bmatrix} \frac{1}{\lambda^2} & 0 & 0 \\ 0 & \frac{1}{\mu^2} & 0 \\ 0 & 0 & \lambda^2\mu^2 \end{bmatrix} - P \begin{bmatrix} 1 & 0 & 0 \\ 0 & 1 & 0 \\ 0 & 0 & 1 \end{bmatrix} + s_+ \begin{bmatrix} \lambda^2 & 0 & 0 \\ 0 & \mu^2 & 0 \\ 0 & 0 & \frac{1}{\lambda^2\mu^2} \end{bmatrix}. \tag{3.18}$$

Since the lateral large surfaces are stress-free we may eliminate P between the three equations (3.18) and obtain

$$\begin{aligned} t_{\lambda\lambda} &= \left(\lambda^2 - \tfrac{1}{\lambda^2\mu^2}\right)\left(s_+ - s_-\mu^2\right), \\ t_{\mu\mu} &= \left(\mu^2 - \tfrac{1}{\mu^2\lambda^2}\right)\left(s_+ - s_-\lambda^2\right). \end{aligned} \tag{3.19}$$

Comparison with the equations (2.36) from the kinetic theory of rubber shows agreement with respect to the first terms in (3.19), the ones with s_+. However, the s_--terms were absent in the kinetic theory.

Without the s_--terms the stress-stretch relation (3.15) is said to represent a neo-Hookean material. Therefore we may say that the kinetic theory of rubber arrives at the equations for a neo-Hookean material and that it misses the second terms, the ones with s_-.

3.7 Free Energy

We recall from Sect. 2.7 or, in particular, from Fig. 2.5 that the elastic forces $\bar{P}_\lambda$ and $\bar{P}_\mu$ are related to the stresses $t_{\lambda\lambda}$ and $t_{\mu\mu}$, cf. (2.36)

$$\bar{P}_\lambda = L^0_\mu L^0_\nu \frac{1}{\lambda} t_{\lambda\lambda} \quad \text{and} \quad \bar{P}_\mu = L^0_\lambda L^0_\nu \frac{1}{\mu} t_{\mu\mu}. \tag{3.20}$$

On the other hand by the Gibbs equation (2.30) we have

$$\bar{P}_\lambda = \frac{\partial F}{\partial L_\lambda} \qquad \text{and} \qquad \bar{P}_\mu = \frac{\partial F}{\partial L_\mu}. \tag{3.21}$$

With $t_{\lambda\lambda}$ and $t_{\mu\mu}$ given by (3.19) we may thus calculate the free energy F as a function of $\lambda = \frac{L_\lambda}{L^0_\lambda}$ and $\mu = \frac{L_\mu}{L^0_\mu}$ by integration. An easy calculation leads to

$$F = \frac{1}{2}V\left[s_+\left(\lambda^2+\mu^2+\frac{1}{\lambda^2\mu^2}-3\right)-s_-\left(\frac{1}{\lambda^2}+\frac{1}{\mu^2}+\lambda^2\mu^2-3\right)\right], \quad (3.22)$$

where the constant of integration has been chosen so as to make the free energy equal to zero in the undistorted state, where $\lambda = \mu = 1$ holds. V is the volume of the membrane.

We note in passing that the combinations of λ and μ that occur in (3.22) represent the traces of $\boldsymbol{B}$ and $\boldsymbol{B}^{-1}$, cf. (3.17) so that we may write

$$F = \tfrac{1}{2}V\left[s_+\left(\mathrm{tr}\boldsymbol{B}-3\right)-s_-\left(\mathrm{tr}\boldsymbol{B}^{-1}-3\right)\right]. \quad (3.23)$$

This is the "stored energy function" of a Mooney-Rivlin material. Equation (3.23) holds in all frames, not only in those with a diagonal stretch tensor.

Actually both (3.22) and (3.23) should contain an additive function of temperature which we drop since it is not important for our purposes.

From the derivation of the specific form (3.23) of F we see that in the theory of elasticity no note is taken that rubber elasticity is entropy-induced. Indeed, it is not necessary in mechanics to split the stored energy function into an internal energy U and an entropic term $-TS$, nor is this usually done. Many mechanicians do not even realize that their stored energy is the free energy of thermodynamics and has an entropic part.

3.8 Rubber Balloon with the Mooney-Rivlin Equation

In order to derive the pressure-radius characteristic of a balloon we proceed exactly as in Sect. 2.8 − and with the same approximation − but now by use of the Mooney-Rivlin formulae (3.19) rather than the formulae (2.36) of the kinetic theory. Thus, instead of (2.37) we obtain

$$t_{\lambda\lambda} = t_{\mu\mu} = s_+\left(\left(\frac{r}{r_0}\right)^2-\left(\frac{r_0}{r}\right)^4\right)+s_-\left(\left(\frac{r_0}{r}\right)^2-\left(\frac{r}{r_0}\right)^4\right).$$

And instead of (2.39) we get

$$[p] = 2s_+\frac{d_0}{r_0}\left(\frac{r_0}{r}-\left(\frac{r_0}{r}\right)^7\right)\left(1-\frac{s_-}{s_+}\left(\frac{r}{r_0}\right)^2\right). \quad (3.24)$$

We plot this function for the values $s_\pm$ given in (3.16) and represent the graph in Fig. 3.4 as the solid curve. Inspection shows that there are two ascending branches now just like those exhibited by experiments, cf. Fig. 1.4. Therefore we are happy and shall proceed − in Chap. 5 − to investigate balloons.

First, however, in Chap. 4 we shall study a biaxially loaded *plane* Mooney-Rivlin membrane.

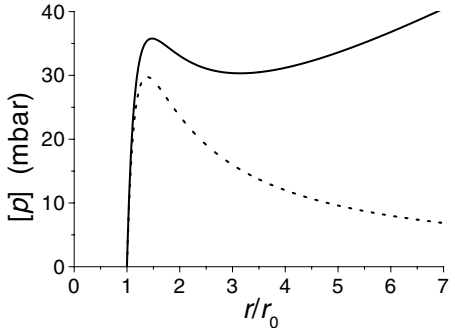

Fig. 3.4. Pressure-radius characteristic of a balloon according to non-linear elasticity of a Mooney-Rivlin material. Dashed curve: Prediction of the kinetic theory of rubber, cf. Fig. 2.7. Both curves for $d_0/r_0 = 0.8 \cdot 10^{-2}$

3.9 Surface Tension

In Chap. 1 a rough-and-ready argument has given us equation (1.1) for the pressure-radius relation of a balloon. σ in that equation is the surface tension and we intimated that it could depend on the radius. And now, having calculated the proper pressure-radius relation of a balloon in (3.24), we may identify the surface tension by comparing the equations (1.1) and (3.24). We obtain

$$\sigma = \frac{1}{2} s_+ d_0 \left(1 - \left(\frac{r_0}{r}\right)^6\right) \left(1 - \frac{s_-}{s_+} \left(\frac{r}{r_0}\right)^2\right). \tag{3.25}$$

A plot of this function − with $d_0 = 0.2$ mm, $s_+ = 3$ bar and $s_- = 0.3$ bar − is shown by the solid line in Fig. 3.5. We see that, as expected, σ is strongly dependent on r, so that for rubber balloons there is no great benefit to be had from writing $[p] = \frac{4\sigma}{r}$.

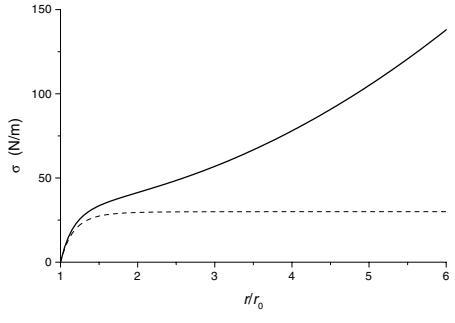

Fig. 3.5. The dependence of surface tension on the radius of a balloon Mooney-Rivlin (solid). Kinetic theory (dashed)

The dotted line in the figure represents the curve predicted by the kinetic theory, i.e. for $s_- = 0$. In that case σ is still dependent on r but over a large range of radii it remains constant. In that range σ has the value $\sigma \approx 30\frac{\mathrm{N}}{\mathrm{m}}$ which is 400 times the value of the surface tension of water and 1200 times the value for a soap bubble. By (2.39) the coefficient s_+ which − according to (3.25) − determines the surface tension is itself determined by the number density of chains in the rubber membrane.

In a manner of speaking we may say that even the Mooney-Rivlin balloon "tries" to approach a constant value of surface tension in the range where the solid curve in Fig. 3.5 flattens and the pressure-radius curve decreases, cf. Fig. 3.4. In that range the simple "$\frac{1}{r}$-law" for the pressure exerts its influence. However, both for large and small radii, the constitutive properties of rubber prevail over the purely geometric tendencies that lead to $[p] = \frac{4\sigma}{r}$.

3.10 Cylindrical Balloon

There is no such thing as a cylindrical balloon, of course, since a balloon must be closed at the ends. What we *can* realize is a cigar-shaped membrane and, if the membrane is long enough, it can be proved that the force balance on the cylindrical part is not noticeably affected by the ends. We proceed under that approximation.

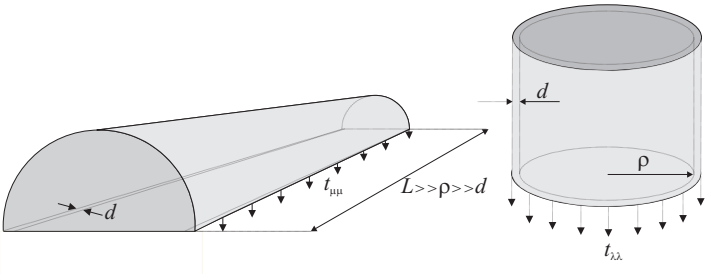

Fig. 3.6. Force balance on a cylindrical balloon of length L, radius $\rho \ll L$, and thickness $d \ll \rho$. $t_{\mu\mu}$ – hoop stress, $t_{\lambda\lambda}$ – axial stress

The pressure jump across the membrane is denoted by $[p]$. We may then write the balance of forces on the halves of the balloon as follows, cf. Fig. 3.6.

$$\text{Radial equilibrium } 2L\ d\ t_{\mu\mu} = \ [p]L\ 2\rho$$

$$\text{Axial equilibrium } \ 2\pi\ \rho d\ t_{\lambda\lambda} = [p]\pi\rho^2.$$

Hence follows

$$[p] = \frac{d}{\rho} t_{\mu\mu} = 2\frac{d}{\rho} t_{\lambda\lambda}, \tag{3.26}$$

so that the hoop stress $t_{\mu\mu}$ is twice as big as the axial stress $t_{\lambda\lambda}$. Equation (3.26) is known to mechanical engineers as the *boiler formula*; they use it for estimating the stresses in cylindrically shaped pressure vessels, not balloons!

In order to obtain a relation between axial stretch $\lambda = \frac{L}{L_0}$ and hoop stretch $\mu = \frac{\rho}{\rho_0}$ we insert (3.19) into $(3.26)_2$ and solve for λ.

$$\lambda(\mu) = \sqrt{\frac{1}{2}\frac{K\mu^2 - \frac{1}{\mu^2}}{2K+\mu^2} + \sqrt{\left(\frac{1}{2}\frac{K\mu^2 - \frac{1}{\mu^2}}{2K+\mu^2}\right)^2 + \frac{K\frac{1}{\mu^2}+2}{2K+\mu^2}}}, \tag{3.27}$$

where $K = -\frac{s_+}{s_-}$. Figure 3.7_{left} shows a graph of this relation for the value $K = 10$ that conforms to (3.16). Inspection of the figure shows that the length of the balloon is largely unaffected by an increase of radius both for small and large radii. If we use (3.26) to plot $[p]$ as a function of μ we obtain the non-monotonic graph of Fig. 3.7_{right}. The analytic form of that function is given by

$$\frac{[p]}{2\,|s_-|\;d_0/\rho_0} = \frac{1}{\lambda\mu^2}\left(\lambda^2 - \frac{1}{\lambda^2\mu^2}\right)\left(K+\mu^2\right). \tag{3.28}$$

It is interesting to note that the pressure becomes independent of the radius as $\mu = \rho/\rho_0$ grows. But then, for large values of ρ our approximation becomes precarious: Indeed, since $\lambda = L/L_0$ tends to a constant for growing μ, cf. Fig. 3.7_{left}, we may soon enter a range where $L \gg \rho$ is violated even though $L_0 \gg \rho_0$ was good in the undistorted state.

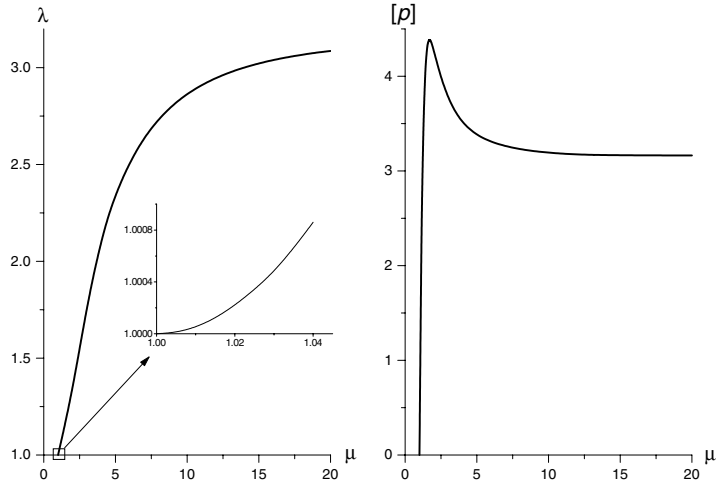

Fig. 3.7. The plots $\lambda = \lambda(\mu)$ and $[p] = [p](\mu)$ for a cylindrical balloon with $K = -\frac{s_+}{s_-} = 10$

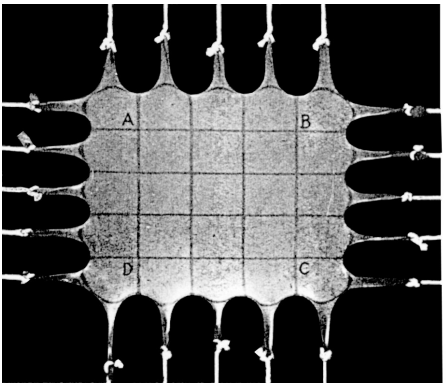

f_1 (gm.)	f_2 (gm.)	λ_1	λ_2
100	100	$1{\cdot}08_8$	$1{\cdot}08_8$
100	200	$0{\cdot}99_6$	$1{\cdot}30_5$
200	200	$1{\cdot}21_3$	$1{\cdot}19_3$
300	200	1·55	$1{\cdot}06_8$
300	100	1·66	$0{\cdot}88_2$
300	300	1·41	$1{\cdot}36_4$
100	400	0·80	2·04
200	400	$0{\cdot}95_6$	$1{\cdot}95_3$
300	400	1·24	1·83
400	400	1·65	$1{\cdot}65_4$
400	500	1·50	2·12
500	500	1·97	1·94
500	300	2·31	1·10
500	200	2·43	$0{\cdot}85_8$
500	100	2·48	$0{\cdot}73_6$

Fig. 3.8. Treloar's biaxial dead-loading experiment

3.11 Treloar's Biaxial Experiment

While the Mooney-Rivlin equations (3.19) with the proper constants $s_\pm$ allow us to draw a correct pressure-radius curve for a balloon, this is not the only – not even the first – success of the Mooney-Rivlin equations. The first confirmation of the Mooney-Rivlin equations came in the mid-forties. In 1947 Treloar published a paper in which he reported results of biaxial dead-loading experiments on a rubber sheet, cf. Fig. 3.8.

Assuming that the sheet was isotropic, Treloar used his 15 measurements to place the 30 open circles into a $(t_{\lambda\lambda}, \lambda^2 - \frac{1}{\lambda^2\mu^2})$-diagram, cf. Fig. 3.9_{left}. This particular plot was chosen in order to check the validity – or otherwise – of the kinetic theory of rubber. Indeed, according to (3.19), if the kinetic theory were correct – i.e. if s_- were equal to zero – we should have $t_{\lambda\lambda} = (\lambda^2 - \frac{1}{\lambda^2\mu^2})s_+$ and therefore Treloar's circles should all lie on a straight line through the origin with the slope s_+, irrespective of the load $\bar{P}_\mu$ in the μ-direction.

What Treloar observed, however, cf. Fig. 3.9_{right}, was a fan-shaped *family of curves*, one curve for each value of $\bar{P}_\mu$. The fact that the fan occurs – rather than a single line – indicates that the kinetic theory of rubber does not properly represent the properties of rubber.

Treloar duely points out that his experiments prove the kinetic theory to be deficient, and he decides to test the alternative formula proposed by Mooney. Mooney's stress-stretch relation for rubber is represented by (3.19).[2] In order to determine the constants $s_\pm$ we solve the two equations (3.19) for $s_\pm$ and obtain, in Treloar's notation

[2] It has become common practice to call these equations the Mooney-Rivlin equations, because Rivlin has firmly installed the Mooney proposition into the theory of non-linear elasticity.

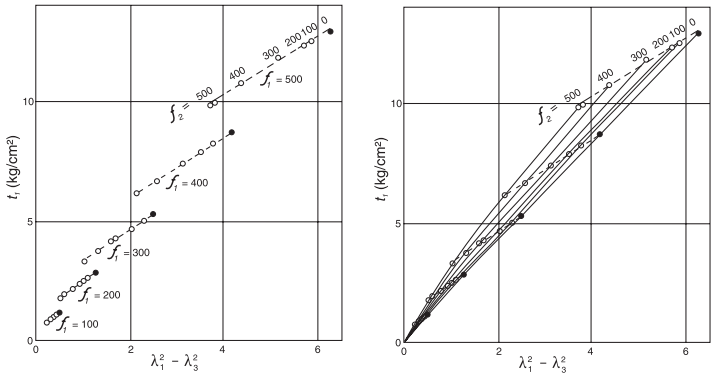

Fig. 3.9. Left: Open circles: Treloar's graphical representation of the measurements reported in Fig. 3.8. Solid circles: Measurements of Treloar for uniaxial tension (not reported in the table of Fig. 3.8). Right: Graphs of $t_{\lambda\lambda}$ vs. $\lambda^2 - \frac{1}{\lambda^2\mu^2}$ for fixed values of $\bar{P}_\mu$ as indicated. [Note that Treloar's notation and ours are different. They correspond to each other according to the following list $(f_1,\, f_2,\, \lambda_1,\, \lambda_2,\, \lambda_3,\, t_1) \hat{=} \left(\bar{P}_\lambda,\, \bar{P}_\mu,\, \lambda,\, \mu,\, \frac{1}{\lambda\mu},\, t_{\lambda\lambda}\right)$. The cross-sectional areas on which f_1 and f_2 are applied are equal to $L_\mu^0 L_\nu^0 = L_\lambda^0 L_\nu^0 = 0.0985$ cm^2 in the undistorted state.]

$$-s_- = \frac{1}{0.0985}\frac{1}{\lambda_2^2-\lambda_1^2}\left(\frac{f_1\lambda_1}{\lambda_1^2-\frac{1}{\lambda_1^2\lambda_2^2}} - \frac{f_2\lambda_2}{\lambda_2^2-\frac{1}{\lambda_1^2\lambda_2^2}}\right),\quad s_+ = s_-\,\lambda_2^2 + \frac{1}{0.0985}\frac{f_1\lambda_1}{\lambda_1^2-\frac{1}{\lambda_1^2\lambda_2^2}}. \tag{3.29}$$

If we use the experimental data of Fig. 3.8 we obtain values for $s_\pm$ as in the following table, where the first double row indicates the loads f_1 and f_2, in grams (!); after all Treloar published in 1947.

Table 3.1. $s_\pm$ calculated from (3.29) with the data of Fig. 3.8

	100 200	300 200	300 100	100 400	200 400	300 400	400 500	500 300	500 200	500 100
$s_-\left[\frac{\text{gr}}{\text{cm}^2}\right]$	−200	−379	−337	−250	−292	−251	−171	−221	−245	−168
$s_+\left[\frac{\text{gr}}{\text{cm}^2}\right]$	2186	1884	1946	2028	1981	1969	2059	1996	1993	2061

The scatter is wild indeed − particularly for s_- − and yet, if we employ the mean values

$$s_- = -251\frac{\text{gr}}{\text{cm}^2} = -0.246 \text{ bar} \quad \text{and} \quad s_+ = 2010\frac{\text{gr}}{\text{cm}^2} = 1.972 \text{ bar}$$

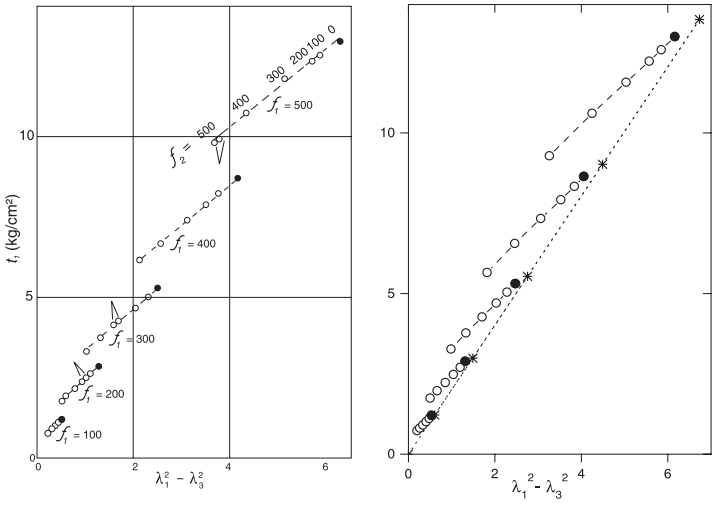

Fig. 3.10. Left: Experimental results as in Fig. 3.9 (scale changed!). Right: Results of calculation for a Mooney-Rivlin material with $s_+ = 2010$ gr/cm^2, $s_- = -251$ gr/cm^2, see text

we may use the equations (3.19) to construct − largely numerically − a diagram like that of Fig. 3.9$_{left}$. This diagram is shown in Fig. 3.10. Comparison with the experimental dots of Fig. 3.9 shows excellent agreement and so Treloar was able to say: "Detailed comparison shows a very close quantitative correspondence between the theoretical and the experimental points". In this manner Treloar firmly established the validity and usefulness of the Mooney-Rivlin stress-stretch relation.[3]

The straight line in Fig. 3.10$_{right}$ − marked by asterisks − corresponds to the kinetic theory. And the black dots correspond to a Mooney-Rivlin material in uniaxial tension, i.e. with $f_2 = 0$. It follows that the kinetic theory is not altogether bad for uniaxial stress-stretch experiments; this circumstance has recommended the kinetic theory to the early researchers.

As we have mentioned, Treloar assumed isotropy when constructing the plots of Fig. 3.9. And yet his experimental results show that equal dead loads $f_{1,2}$ do not always lead to equal stretches $\lambda_{1,2}$. This is why two adjacent points appear for $f_{1,2} = 500$, $f_{1,2} = 300$ and $f_{1,2} = 200$, cf. the chevrons in Fig. 3.10$_{left}$. Treloar does not mention this oddity nor should we, if it were not for the fact that in the later literature this double occurence of what should by rights be a single dot has been misinterpreted and has led to a misunderstanding. We shall explain later, in Sect. 4.11, when the point becomes relevant.

[3] The data reported are for swollen rubber. Treloar was less enthusiastic about the validity of the Mooney-Rivlin relation for dry rubber.